

Experimental Test of a UWB Closed-Form EGN Model

Original

Experimental Test of a UWB Closed-Form EGN Model / Jiang, Y., Bosco, G., Nespola, A., Tanzi, A., Piciaccia, S., Zefreh, M.R., Forghieri, F., Poggiolini, P.. - ELETTRONICO. - (2023). (2023 IEEE Photonics Conference (IPC) Orlando, FL, USA 12-16 November 2023) [10.1109/ipc57732.2023.10360723].

Availability:

This version is available at: 11583/2986509 since: 2024-03-03T15:03:58Z

Publisher:

IEEE

Published

DOI:10.1109/ipc57732.2023.10360723

Terms of use:

This article is made available under terms and conditions as specified in the corresponding bibliographic description in the repository

Publisher copyright

IEEE postprint/Author's Accepted Manuscript

©2023 IEEE. Personal use of this material is permitted. Permission from IEEE must be obtained for all other uses, in any current or future media, including reprinting/republishing this material for advertising or promotional purposes, creating new collecting works, for resale or lists, or reuse of any copyrighted component of this work in other works.

(Article begins on next page)

Experimental Test of a UWB Closed-Form EGN Model

Yanchao Jiang¹, Gabriella Bosco¹, Antonino Nespola², Alberto Tanzi³, Stefano Piciaccia³,
Mahdi Ranjbar Zefreh³, Fabrizio Forghieri³, Pierluigi Poggiolini¹

1. OptCom, DET, Politecnico di Torino, C.so Duca Abruzzi 24, 10129, Torino, Italy

2. LINKS Foundation, Via Pier Carlo Boggio 61, 10138, Torino, Italy

3. CISCO Photonics Italy srl, via Santa Maria Molgora 48/C, 20871, Vimercate (MB), Italy
pierluigi.poggiolini@polito.it

Abstract—We present an experimental test of a closed-form ultra-wide-band EGN model, carried out over a 5-span full C+L transmission line. We found quite good correspondence between predicted and measured performance. We then present a theoretical case-study with the S-band being added to the set-up.

Keywords—EGN-model, GN-model, UWB, ISRS, Raman

I. INTRODUCTION

Incorporating physical-layer models into optical networking design and control is crucial. Successful physical-layer models (PLMs) include the widely used GN and EGN models. Recently, demands on PLMs have escalated, requiring quicker computations for real-time optimization and management, plus support of ultra-wide-band (UWB) C+L and in prospect C+L+S systems [1], [2]. To meet these demands, real-time UWB non-linear interference (NLI) closed-form models (CFMs) have been developed, accounting for the frequency-dependence of all key system parameters and including Inter-channel Raman scattering (ISRS). UCL, and PoliTo with CISCO, developed independently such CFMs based on the GN and EGN models. Differences exist in features and final form. See [3] (and refs. therein) for the UCL CFM, and [4] (and refs. therein) for the CISCO-PoliTo CFM. In view of the possible use of the CISCO-PoliTo CFM (henceforth “CFM”) in deployed networks, we conducted several validation experiments on a 5-span C+L system, testing different propagation conditions. The CFM consistently aligned quite well with experimental results.

In this paper we first discuss this validation effort. Then, we use the CFM to predict the performance of the experiment set-up in the case the S-band was added to it. Such case-study shows the usefulness of flexible and efficient tools like this CFM in the process of designing and optimizing future UWB systems.

II. THE EXPERIMENTAL SETUP

The setup is shown in Fig.1(a). It consisted of 61 channels in C-band, from 191.8 to 195.9 GHz, and 67 channels in L-band, from 186.2 to 190.8 GHz. The C+L WDM comb was generated by shaping ASE noise through programmable optical filters, emulating 52GBaud channels spaced 68.75GHz, roll-off 0.1. For performance measurement, each emulated channel was replaced in turn by an actual PM-16QAM channel.

The line consisted of 5 spans of SMF with 86km length. The line was instrumented so that both the full signal spectrum and

the spectrally resolved OSNR could be measured at each one of the red and green probing points shown in Fig.1(a), numbered from “0” to “5”. This way, the gain and noise figure of each EDFA could be measured vs. frequency, while the system was operating. The receivers were separate C and L-band units. They provided the constellation SNR after DSP.

The launched WDM spectrum into the first span could be arbitrarily shaped by means of programmable optical filters. Each amplifier could be controlled as to its gain and tilt, so that quite different propagation conditions could be imposed.

The fibers were SMF G652D. The five spans were characterized as for their attenuation and dispersion vs. frequency. The fiber non-linearity coefficient γ was measured by means of a dedicated pump-probe experiment and found to be about 1.25 1/(W km) at 192 THz. We then used Eq. (4) from [5] to account for the frequency-dependence of γ . Note that Eq. (4) [5] also provides different values of γ for SPM and XPM, which we took into account in the CFM. Regarding ISRS, the Raman gain spectrum was measured at a pump frequency of 206.5 THz and then translated to different pump frequencies according to Eqs. (37)-(39) in [6].

III. EXPERIMENTAL RESULTS

Our goal was to compare the experimental GSNR (GSNR_{exp}) with the GSNR estimated through the CFM (GSNR_{CFM}) on all channels. GSNR_{exp} was found as follows: the Rx provided SNR_{exp} , i.e., the SNR measured by the Rx on the constellation, after DSP. SNR_{exp} relates to GSNR_{exp} as follows:

$$\text{GSNR}_{\text{exp}} = \text{SNR}_{\text{exp}} \cdot (1 - \text{SNR}_{\text{exp}}/\text{SNR}_{\text{bb}})^{-1}$$

where SNR_{bb} is the measured constellation SNR in back-to-back (no ASE) which accounts for the internal Tx-Rx noise. We found $\text{SNR}_{\text{bb}} = 19.9$ dB for both the C and L band Tx-Rx pairs.

For GSNR_{CFM} , the non-linearity noise (NLI) was estimated using the CFM, based on the measured launched signal power spectrum into each span. We also estimated NLI using the full-fledged, numerically integrated EGN model, upgraded for UWB support, to obtain GSNR_{EGN} .

Fig.1(b) shows the results of the comparison among GSNR_{exp} , GSNR_{CFM} and GSNR_{EGN} . It also shows the OSNR measured at the receiver, which accounts just for signal and ASE noise (but no NLI). In the test, the launch power was optimized to try to maximize the overall system throughput, which was 53Tb/s. Fig.1(b) shows quite good correspondence between all three GSNRs, in both bands.

We carried out the CFM validation in several other operating conditions, such as targeting flatter GSNR or much more highly non-linear regimes, which we cannot report here due to lack of

This work was partially supported by: Cisco Systems through the ITROCS research contract; the PhotoNext Center of Politecnico di Torino; the European Union under the Italian National Recovery and Resilience Plan (NRRP) of NextGenerationEU, partnership on “Telecommunications of the Future” (PE00000001 - program “RESTART”).

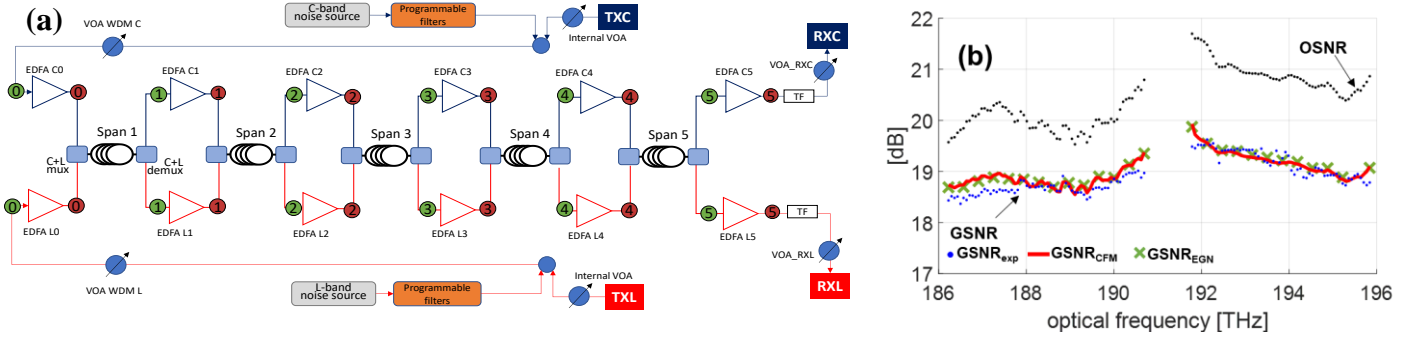


Fig. 1 (a): schematic of the C+L line experiment. VOA: variable optical attenuator. TF: tunable filter. (b): plot of measured OSNR (ASE only), measured $GSNR_{exp}$, closed-form-model prediction $GSNR_{CFM}$, and EGN model prediction $GSNR_{EGN}$ for a system scenario aiming at maximizing throughput.

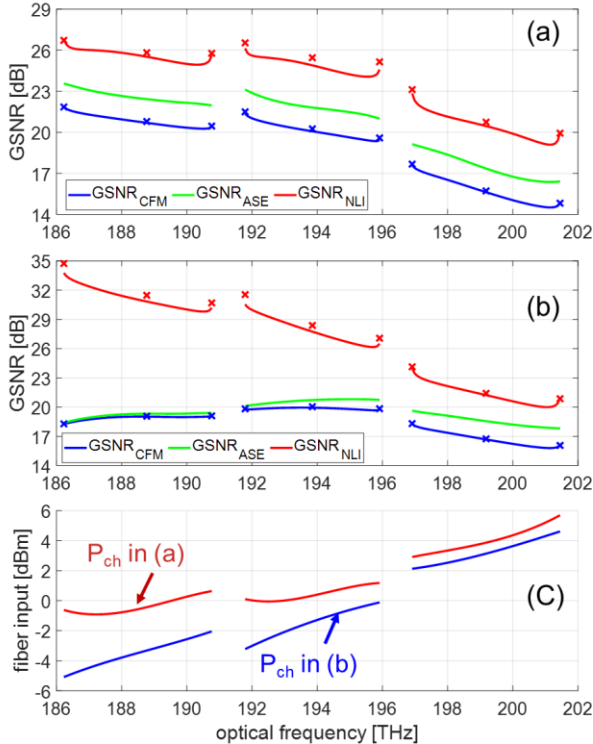


Fig. 2 (a) and (b): closed-form-model GSNR prediction ($GSNR_{CFM}$, solid lines) and EGN model prediction ($GSNR_{EGN}$, markers) for a C+L+S system similar to the experiment of Fig.1, aiming at (a) NLI being about $\frac{1}{2}$ of ASE noise and (b) maximizing throughput. (c): launch power profiles optimized to obtain the conditions for (a) and (b).

space. $GSNR_{CFM}$ was always within ± 0.6 dB of $GSNR_{exp}$ and almost coincident with $GSNR_{EGN}$. These result, in our view, suggest that the CFM is quite reliable, even in challenging scenarios such as the one used for testing.

IV. ADDING THE S-BAND TO THE SET-UP

We emulated with the CFM the 5-span test-bed shown in Fig.1(a), using its parameters characterized experimentally, while adding the S-band (196.9THz to 201.5THz), using same format, symbol rate, spacing, etc., as used for the C and L bands. Regarding amplifiers, we assumed 7dB noise figure in both L and S bands and 5dB in the C band. By means of the CFM we carried out various optimizations. In Fig.2(a) we aimed at keeping the level of NLI at about $\frac{1}{2}$ that of ASE, a condition where each channel GSNR approaches a local maximum vs.

launch power. The plot clearly shows that the S-band has substantial penalty due to the challenging scenario that includes C+L+S, with substantial ISRS power transfer from the S-band to C and especially L band. Note also that both loss and non-linear coefficients are higher in the S-band. A much more balanced GSNR can be achieved by setting as goal the maximization of the total throughput, as shown in Fig.2(b).

In selected cases we checked the accuracy of the CFM vs. the full-fledged EGN-model (see markers in Fig.2) with good agreement. Studies are ongoing using the CFM on C+L+S systems, where various types of optimizations can be carried out thanks to the speed of the CFM.

V. CONCLUSION

We conducted a dedicated experiment using a 5-span C+L setup to evaluate the accuracy of a closed-form non-linearity model (CFM), developed jointly by CISCO and PoliTo. The CFM takes into account the impact of ISRS and the frequency-dependence of all fiber parameters. Our findings indicate that the CFM shows quite good accuracy across several propagation scenarios. We found that possible discrepancy in predicting the system GSNR is perhaps mostly due to uncertainty in characterizing amplifiers, fibers, and other components, rather than to the CFM's inaccuracy in assessing NLI. In a C+L+S case-study we showed the usefulness of efficient tools like CFM in the process of designing and optimizing future UWB systems.

In conclusion, from the perspective of non-linearity modeling, the CISCO-PoliTo-CFM exhibits a good level of reliability throughout the entire C+L band, as well as real-time computation speed, suggesting it could be fast and accurate enough for possible use in actual networks.

REFERENCES

- [1] J. Renaudier et al., "Devices and Fibers for Ultrawideband Optical Communications," Proc. IEEE, vol. 110, no. 11, pp. 1742-1759, 2022.
- [2] T. Hoshida et al., "Ultrawideband Systems and Networks: Beyond C + L-Band," Proc. IEEE, vol. 110, no. 11, pp. 1725-1741, 2022.
- [3] H. Buglia et al., "A Closed-Form Expression for the Gaussian Noise Model in the Presence of Inter-Channel Stimulated Raman Scattering Extended for Arbitrary Loss and Fibre Length," JLT, vol. 41, no. 11, pp. 3577-3586, 2023.
- [4] P. Poggiolini and M. Ranjbar-Zefreh, "Closed Form Expressions of the Nonlinear Interference for UWB Systems," ECOC 2022, p. Tu1D.1.
- [5] M. Santagiustina et al., "Theory of slow light enhanced four-wave mixing in photonic crystal waveguides," Opt. Expr., v. 18, n. 20, pp. 21024, 2010.
- [6] K. Rottwitt et al., "Scaling of the Raman gain coefficient: applications to germanosilicate fibers," JLT, vol. 21, no. 7, pp. 1652-1662, 2003.

